Chapter 4

GaN Epitaxial Growth on Silicon (1 1 1) Substrates

4.1 Introduction

Group-III-nitride semiconductor devices are usually grown on sapphire or SiC substrates. These are either insulating or very expensive and not available in large diameter. Recently, silicon as a substrate has attracted much attention for the epitaxial growth of group-III-nitride semiconductors because of its low cost, well-conducting, large size in large diameters up to 12 inches and potential in the integration of microelectronic and optoelectronic devices. However, large difference in in-plane thermal expansion coefficient (56%) [30, 31] between GaN and Si, which causes a large tensile stress in the GaN epilayers during cooling down process resulting in cracked layers especially in MOVPE system [32]. In MBE grown samples the critical thickness is higher than in MOVPE grown because of the lower growth temperature. The large difference in the lattice constant of the Si and GaN yields 16.9% mismatch resulting in a high dislocation density in the GaN layer. To overcome this problem, various types of buffer layers such as 3C-SiC [33], AlN [34], γ-Al_2O_3 [35], β-Si_3N_4 [36] and GaN nanorods [37] have been used to reduce the mismatch between GaN and Si. To date, among all the reported buffer layers for GaN on Si, the AlN buffer layer approach yields the best results reported in the literature, leading to the demonstration of high-brightness light-emitting diodes on Si. Moreover, when exposed to reactive nitrogen radicals, the silicon surface has a tendency to form an amorphous silicon nitride (SiN) layer, which deteriorates the epitaxial layers. To prevent amorphous SiN formation, a few monolayers (ML) aluminum pre-seeding layer were deposited on the surface [36, 38, 39]. GaN nanorod is a promising buffer layer for overgrowing GaN on Si. The characteristics of GaN nanorods will discuss latter.

One-dimensional structures (nanowires or nanorods) of nanometer-scale GaN are known

to have great prospects in fundamental physical science and novel technological applications. There are several interesting reports that catalyst-free, RF plasma-assisted molecular-beam epitaxy (RF-MBE) can be applied to grow vertically self-aligned wurtzite III-nitride GaN, AlGaN, InN (nanorods, nanocolumns, nanowires, nanopillars) on Si (1 1 1), sapphire (0 0 0 1), and Si (0 0 1) substrates [40]. Recently, the RF-MBE-grown III-nitride nanorods arrays exhibit some promising properties for growing dislocation- and strain-free III-nitride. Especially, the III-nitride nanorod was grown on large lattice mismatch substrate and the grown nanorods are fully relaxed, resulting in strain-free, dislocation-free single crystal. The self-assembled GaN nanorods are employed as a compliant template for overgrowth of strain-free GaN [41]. The strain extended structure defects would be located at the nanorods bottom interface. Moreover, one-dimensional electroluminescent device using GaN or AlGaN nanorod templates have been demonstrated [42].

In this chapter, the simultaneous AlN/α-Si_3N_4 buffer structure with Al pre-seeding layer and novel substrate engineering (GaN-nanorods buffer) was applied to grow high quality GaN epilayer on Si (111) substrates. We investigated the effect of Al pre-seeding layer deposition time on the quality of the GaN epitaxial layer. After Al pre-seeding layer deposition, we found the crystal α-Si_3N_4 layer was accompanied with AlN growth process. Crack free GaN layers were demonstrated by using simultaneous AlN/α-Si_3N_4 buffer structure. In addition, we also investigated the formation of high-quality, hexagonal and vertical GaN nanorods buffer grown by a self-assembled mechanism on Si (1 1 1) substrates at different molecular beam epitaxy condition. We have used the GaN nanorods buffer technique to develop strain-free GaN by MBE and MOCVD-overgrown GaN.

4.2 Growth procedure of the GaN epitaxial layer and nanorods on Si (1 1 1)

The growth of GaN epitaxial layer was carried out on Si (1 1 1) substrates by RF-MBE

(ULVAC MBE system). Two-inch Si (1 1 1) wafers (p-type doping) were chemically cleaned by 10% HF without DI water rinsed for suppressing oxide formation. Clear (7×7) surface reconstruction confirmed by high-energy electron diffraction (RHEED) at ~830℃. To prevent amorphous SiN formation on the Si surface, different deposition time of Al pre-seeding layers were covered on Si surface. The Al pre-seeding layer was deposited on Si surface at 700℃ and annealing for 150 sec. The AlN was grown at gradation of temperature from 700 to 820 ℃ by temperature grading method to form the simultaneous crystal α-Si_3N_4 layer during AlN growth process. The ramping rate was 35 ℃/min in grading process. The AlN layer was grown epitaxially at the gradation of 700 ℃ to 820 ℃. The GaN epitaxial layer was grown on simultaneous AlN/α-Si_3N_4 buffer structure at 790 ℃. The sample with simultaneous AlN/α-Si_3N_4 structure is crack free after 1.2 μm thick GaN epitaxial layer growth. The detail growth parameters are shown in the Table 4-1 and the schematically depicts the growth procedure is shown in Fig. 4-1.

The GaN nanorods were directly grown on Si (1 1 1) substrates at N-rich condition instead of forming a nucleation layer such as Al pre-seeding layer and high temperature AlN buffer layer prior to the GaN growth. Two series of the samples were designed to investigate the effect of the growth temperature and Ⅴ/Ⅲ ratio. The detail growth parameters are shown in the Table 4-2.

We grew the GaN nanorods buffer layers for MBE and MOCVD overgrowing GaN. Self-assembled GaN nanorods were grown under N-rich condition at 900℃. The nitrogen flow rate and RF input power of the two plasma generators were maintained at 4 sccm / 500W and 1.5 sccm / 500W and the beam equivalent pressure (BEP) of the gallium was fixed at 2.0× 10^{-7} torr during GaN nanorods growth.

Subsequently, in the part of the MBE-overgrown GaN, the GaN film was directly overgrown on self-assembled nanorods under Ga-rich condition at 800℃. The BEP of the gallium was fixed at 3.6×10^{-7} torr and the nitrogen flow rate and RF input power of the two

plasma generators were maintained at 4 sccm / 500W and 1.5 sccm / 500W.

In the part of the MOCVD-overgrown GaN, trimethylgallium (TMGa) and NH_3 were employed as the reactant source materials for Ga and N, respectively. The temperature of GaN nanorods template was ramped from 25℃ to 1150℃ in NH_3, H_2 and N_2 atmosphere. Two steps GaN growth was applied. The 1st step of GaN was grown at 1150℃ with the growth rate of 1.6 μm/hr, and the 2nd step of GaN was grown at 1150℃ with the growth rate of 3.0 μm/hr. Fig. 4-2 shows schematic diagrams of the overgrown GaN on self-assembled GaN nanorods.

4.3 Characteristics of the GaN epitaxial layer and nanorods on Si (1 1 1) substrate

Si wafers were further thermally degassed to remove the fluorine and remaining oxide layer on the surface at high temperature. Surface reconstruction was observed by the evolution of RHEED patterns during the growth process. Fig. 4-3 (a) shows the clear (7×7) surface reconstruction at 830℃. Fig. 4-3 (b) to (d) show the RHEED pattern with deposition time (15s, 30s and 45s) of Al pre-seeding layer. The Si (1 1 1) 7×7 pattern fade out as the deposition time of Al pre-seeding layer increased. The AlN pattern without Al pre-seeding layer is dim (Fig. 4-3 (e)), which means AlN layer was difficult to grow on Si surface without Al pre-seeding layer. On the contrary, the AlN pattern with 45s Al pre-seeding layer is clear, as shown in Fig. 4-3 (f). Streaky (1×1) RHEED pattern indicates 2D growth and flat surface morphology for GaN epitaxial layer, as shown in Fig. 4-3 (g).

The crystal quality of GaN epitaxial layer with various deposition time of Al pre-seeding layer on Si (1 1 1) substrate was characterized by HRXRD ω-scan of symmetric (0 0 0 2). Fig. 4-4 shows the full widths at half-maximum (FWHM) value of the x-ray rocking curve as a function of the deposition time of Al pre-seeding layer. The crystal quality of GaN epitaxial

layer becomes better with increasing the deposition time of Al pre-seeding layer, but worse at 60s Al pre-seeding layer deposition. It was found that the optimum Al deposition time is 45s at $Al_{BEP}=2.5\times10^{-8}$ torr. The size of 2D Al-islands increase with deposition time of Al pre-seeding layer increasing. Larger size of 2D Al-islands could cover almost all Si surface. On the 2D Al-island, active nitrogen would react with Al-island to form high quality AlN layer; but some free Si surface without 2D Al-island covered, amorphous SiN was formed, which deteriorates subsequent AlN layer and GaN layer. On the other hand, the crystal quality of GaN epilayer is worse at 60s Al pre-seeding layer deposition time, because the Al pre-seeding layer did not all react with nitrogen radical to form uniform AlN layer.

The GaN epitaxial layer grown on Si (1 1 1) was investigated by HRXRD in the θ-2θ scan mode as shown in Fig. 4-5. The diffraction peak at 34.59° and 72.96° is intense and is identified as wurtzite GaN (0 0 0 2) and (0 0 0 4) diffraction. The diffraction peak near 31.1° and 64.85° is attributed to the (0 0 2) and (3 0 3) diffraction of the α-Si_3N_4 layer, which was formed during AlN growth process. The crystal α-Si_3N_4 (0 0 0 1) lattice coincidently matches (1:2) with the Si (1 1 1), which can reduce the lattice mismatch.

Fig. 4-6 shows the surface SEM morphology of the GaN epitaxial layer with AlN/α-Si_3N_4 buffer structure on Si (1 1 1). The crack free surface of 1.22 μm thick GaN is found in this sample even at the scale as large as several hundreds of microns.

In order to improve the crystal quality of GaN epitaxial layer on Si (1 1 1) further, we used the method of AlN-IL inserted in GaN epitaxial layer, which have been studied in Chap. 3. Fig. 4-7 shows the HRXRD ω-scan profile of symmetric (0 0 0 2) and asymmetric (1 0 $\bar{1}$ 2) diffraction for the GaN epitaxial layer with AlN-IL on Si (1 1 1). The full-width at half-maximum (FWHM) of symmetric (0002) and asymmetric (10-12) are 1128 arcsec and 2724 arcsec. This result is comparable with other groups [43, 44].

The PL measurement is performed at 13K to investigate the optical properties of the GaN epitaxial layer on Si (1 1 1) as shown in Fig. 4-8. The 13K-PL spectrum shows a dominant

emission peak at 3.46eV, which is attributed to the neutral-donor-bound exciton (D^oX) of the wurtzite GaN epilayer. The FWHM of the D^oX peak of the GaN is measured to be 20 meV. The defect-related yellow-band emission centered at 2.2eV is very weak.

The self-assembled GaN nanorod was used as a buffer for further improving the crystal quality of GaN on Si. The self-assembled GaN nanorod grown by RF-MBE at various growth temperatures (750 to 900℃) at a fixed Ⅴ/Ⅲ ratio was discussed. Fig. 4-9 (a) to (d) shows plan view and cross-section view scanning electron microscope (SEM) images of the self-assembled GaN nanorods grown on Si (1 1 1) at growth temperature of 750 to 900℃. The morphology of the self-assembled GaN nanorods grown on Si (1 1 1) depends strongly on the growth temperature. At the low growth temperature (Growth Temp=750℃ or 800℃), the Ⅴ/Ⅲ ratio of the Si (1 1 1) surface was in slight N-rich condition. Consequently, the coalescence phenomenon of individual nanorods into nanorod bundles was observed in Fig. 4-9 (a) and (b). The RHEED pattern indicated a spotty pattern at growth Temp=750℃ or 800 ℃ as shown in Fig. 4-10 (a) and (b). It means individual nanorod bundles were coalesced together to result in rough surface. However, at the high growth temperature (Growth Temp=850℃ or 900℃), excess Ga adatoms could be re-evaporated from the Si (1 1 1) surface. For this reason, the effective Ⅴ/Ⅲ ratio of the Si (1 1 1) surface was in high N-rich condition. No significant coalescence phenomenon of individual nanorods can be found as shown the Fig. 4-9 (c) and (d). And, the hexagonal-shape surface of GaN nanorods was observed. The ellipse-like pattern in RHEED observation (Fig. 4-10 (c) and (d)) corresponds to the superposition of the diffraction by the top (0 0 0 1) plane and the sidewall of GaN nanorod.

Dependence of the GaN nanorods density and diameter on the growth temperature is shown in Fig. 4-11. It shows GaN nanorods density reduces together with a diameter increase. The high growth temperature resulted in the high surface mobility of the Ga adatoms leads to the easier formation of the small size of nucleation seeding site. The height of GaN nanorod

estimated by SEM image is shown in Fig. 4-12, as a function of the growth temperature. With increase of growth temperature, the height of GaN nanorods also increases, which is due to the small size of nucleation seeding sites at high temperature. At equal Ga and N supply, the height of GaN nanorods with small size of nucleation seeding sites is higher than the height of GaN nanorods with large size of nucleation seeding sites.

Fig. 4-13 (a) to (d) shows plan view and cross-section view SEM images of the self-assembled GaN nanorods grown on Si (1 1 1) for different BEP of the gallium from 2.8×10^{-8} to 3.6×10^{-7} torr with fixed amount of active nitrogen at growth temperature of 850℃. With the BEP of the gallium increasing from 2.8×10^{-8} to 2.0×10^{-7} torr (highly N-rich to slightly N-rich) , the density of GaN nanorods reduces together with the diameter of GaN nanorods increase. This phenomenon is the same as above discussion. As a consequence, N-rich condition at the surface may be reached either by increasing the Ⅴ/Ⅲ ratio or by increasing the growth temperatures, although both methods may not be equivalent in terms of nanorods density and size because the later method may increase the Ga adatoms surface mobility. However, the BEP of gallium=3.6×10^{-7} torr at Ga-rich condition, the individual nanorod bundles were coalesced together to form GaN thin film with a hexagonal-shape surface.

In order to estimate the c-axis lattice constant of the GaN nanorods grown at substrate temperature=850℃, the X-ray diffraction (XRD) in the θ-2θ scan mode was performed as shown in Fig. 4-14. The diffraction peak at 34.56^{o} and 72.90^{o} is intense and is identified as wurtzite GaN (0 0 0 2) and (0 0 0 4) diffraction. According to the Bragg diffraction equation ($2\ d\ \sin\theta = n\ \lambda$), the c-axis length of GaN nanorods is 5.1863 Å, which approach the strain-free value of 5.185 Å [45]. The GaN epilayer on Si (1 1 1) substrate contain generally tensile strain. This finding demonstrates self-assembled nanorods are high quality strain-free single crystal.

Figure 4-15 (a) and (b) shows the PL spectra of the GaN nanorods on different Ⅴ/Ⅲ

ratio and growth temperature. The board emission around 3.30 ~ 3.40 eV is considered as GaN nanorods characteristics peak. Samples with the Ⅴ/Ⅲ ratio of the surface from slightly N-rich to highly N-rich (Ga_{BEP} decrease) conditions, the GaN nanorods characteristics peak present the blue-shift to higher energy. The same blue-shift behavior in the characteristics peak of GaN nanorods was also observed in the sample grown with higher temperature (highly N-rich). The blue-shift phenomenon in highly N-rich condition could be attributed to the higher density and smaller diameter of GaN nanorods. The GaN nanorods characteristics peak (3.30 eV) and the D^oX of the GaN film (3.47 eV) was observed in the sample grown under $Ga_{BEP}=2.0\times10^{-7}$ torr at 750℃, which is due to the coalescence phenomenon of individual nanorods into nanorod bundles (Fig. 4-9 (a)). Beside, the defect level emission (DLE) centered at about 2.2eV is not obviously observed in different Ⅴ/Ⅲ ratio and growth temperature samples.

The MBE-overgrown GaN on the self-assembled GaN nanorods was studied. The RHEED exhibited gradual change from a spotty pattern to streak + spotty pattern as shown in Fig. 4-16. The streak + spotty pattern were contributed to flat hexagonal step and the boundary of hexagonal step respectively, which can be confirm by the SEM image of MBE-overgrown GaN on GaN nanorods as shown in Fig. 4-17 (a). The lateral growth with a coalescence process was not easily occurred in the MBE-overgrown GaN with obvious coalescence grain boundary. However, the flat overgrown GaN layers were obtained by MOCVD-grown GaN as shown in Fig. 4-17 (b). It is generally considered that MOCVD growth of GaN has excellent ability of lateral growth.

In order to survey the polarity of overgrown-GaN, 2M KOH solution was used to etch the overgrown-GaN. The MBE overgrown-GaN shows different surface morphology between as-grown and after etching, as shown in Fig. 4-17 (a) and (c). On the contrary, MOCVD overgrown-GaN shows flat surfaces after etching, as shown in Fig. 4-17 (b) and (d). This finding shows the MBE overgrown-GaN is N-polarity, but the MOCVD overgrown-GaN is

Ga-polarity, which fit in with common understanding.

In order to estimate the c-axis lattice constant of the overgrown-GaN on nanorods, the X-ray diffraction (XRD) in the θ-2θ scan mode was performed, as shown in Fig. 4-18. Two peaks are indexed as (0 0 0 2) and (0 0 0 4) of the wurtzite structure of GaN. It is generally considered that the GaN epilayer on Si (1 1 1) substrate contain in-plane tensile strain due to the difference of thermal expansion coefficients. However, according to the Bragg diffraction equation ($2\ d \sin\theta = n\ \lambda$), the c-axis length of MBE-overgrown GaN on nanorods is 5.1848 Å, which approach the strain-free value of 5.185 Å. The biaxial strain was localized at the interface of GaN nanorods and sapphire. These finding suggest that nanorods effectively reduce the biaxial strain. But, the c-axis length of MOCVD-overgrown GaN on nanorods is 5.1921 Å, which means MOCVD-overgrown GaN contain some in-plane compress strain. The GaN grown on Si (1 1 1) with compress strain is a special phenomenon. Detail investigations of this effect have been under the way.

The photoluminescence (PL) measurement was performed at 13K to investigate the optical properties of the MBE-overgrown GaN on self-assembled GaN nanorods, as shown in Fig. 4-19 (a) and (b). Strong excitionic emission is clearly observed at 3.477 eV in two samples, which corresponds to the emission of neural donor bound exciton (D^oX). The PL band at around 3.21 ~ 3.27 eV (MBE-overgrown GaN) is contributed by donor-acceptor-pair (DAP) and conduction –band-acceptor (e-A) [46]. The detail mechanisms have not been understood need further study. In the MBE-overgrown GaN, the defect level emission (DLE) centered at about 2.2eV is not obviously observed, which shows defect density of MBE-overgrown GaN on self assembled is very low. However, the very weak DEL is observed in the MOCVD-overgrown GaN.

4.4 Summary

High quality GaN epitaxial layer on Si (1 1 1) substrate is obtained by introducing a simultaneous AlN/Si_3N_4 buffer structure and AlN-IL by MBE system. The crystal quality of GaN epitaxial layer is improved with increasing the deposition time of Al pre-seeding layer, because the 2D Al-island could avoid the amorphous SiN formation. It was found that the optimum Al deposition time is 45s at $Al_{BEP}=2.5\times10^{-8}$ torr. The simultaneous AlN/α-Si_3N_4 buffer structure could reduce the lattice mismatch due to the crystal α-Si_3N_4 (0 0 0 1) lattice coincidently matches (1:2) with the Si (1 1 1). The GaN epitaxial layer shows a wurtzite structure and exhibits excellent structural and optical properties as evidenced by XRD and PL measurements. The crack free surface of 1.22 μm thick GaN epitaxial layer was obtained by using simultaneous AlN/α-Si_3N_4 buffer structure.

The growth condition dependence on hexagonal phase GaN nanorods, which are vertical to the Si (1 1 1) growth plane, has been investigated. The morphology of GaN nanorods strongly depends on growth condition, i.e. growth temperature, Ⅴ/Ⅲ ratio. With the growth temperature increase, the density of GaN nanorods increase, the diameter of GaN nanorods decrease and the height of GaN nanorods increase, which are due to initial nucleation seeding site. With the BEP of the gallium increasing from 2.8×10^{-8} to 2.0×10^{-7} torr , the density of GaN nanorods reduces together with the diameter of GaN nanorods increase. However, the BEP of gallium=3.6×10^{-7} torr at Ga-rich condition, the individual nanorod bundles were coalesced together to form GaN thin film with a hexagonal-shape surface. As a consequent, we can control the density and diameter of GaN nanorods by growth temperature and Ⅴ/Ⅲ ratio. The board emission around 3.30 ~ 3.40 eV is considered as GaN nanorods characteristics peak. From slightly N-rich to highly N-rich, the GaN nanorods characteristics peak present the blue-shift to higher energy due to the higher density and smaller diameter of GaN nanorods. The self-assembled GaN nanorods are high quality strain-free single crystal as

evidenced by XRD measurement.

The GaN epitaxial layer was grown on novel substrate engineering (nanorods buffer) by MBE and MOCVD. The lateral growth with a coalescence process was not easily occurred in the MBE-overgrown GaN with obvious coalescence grain boundary. However, the flat overgrown GaN layers were obtained by MOCVD-grown GaN. The high quality and strain-free GaN epitaxial layer is grown by using nanorods buffer as evidenced by XRD and PL measurements

Table 4-1 The growth parameters of GaN on Si with AlN/α-Si_3N_4 buffer structure

Step	Growth Parameters
Al pre-seeding layer	Sub. Temp=700 ℃ Deposition time=0 , 15 , 30 , 45 , 60 sec Al_{BEP}=2.5×10^{-8} torr
Simultaneous AlN/α-Si_3N_4 buffer structure	Sub. Temp= gradation of 700 to 820 ℃ Growth time=1 hrs Al_{BEP}=2.5×10^{-8} torr N* Plasma：300W/1.5sccm
GaN epitaxial layer	Sub. Temp=790 ℃ Growth time=3 hrs Ga_{BEP}=3.0×10^{-7} torr N* Plasma 1：500W/4.0sccm N* Plasma 2：500W/1.5sccm

Table 4-2 The growth parameters of self-assembled GaN nanorod growth

Series A. The effect of growth temperature

Sub. Temp. (℃)	**The flux of GaN nanorod growth**
750	Ga_{BEP}=2.0×10^{-7} torr
800	N* Plasma 1：500W/4.0sccm
850	N* Plasma 2：500W/1.5sccm
900	For 120 min

Series B. The effect of Ⅴ/Ⅲ ratio

Sub. Temp. (℃)	**The flux of GaN nanorod growth**
850	Ga_{BEP}=2.8×10^{-8} ~ 3.6×10^{-7} torr N* Plasma 1：500W/4.0sccm, N* Plasma 2：500W/1.5sccm For 120 min

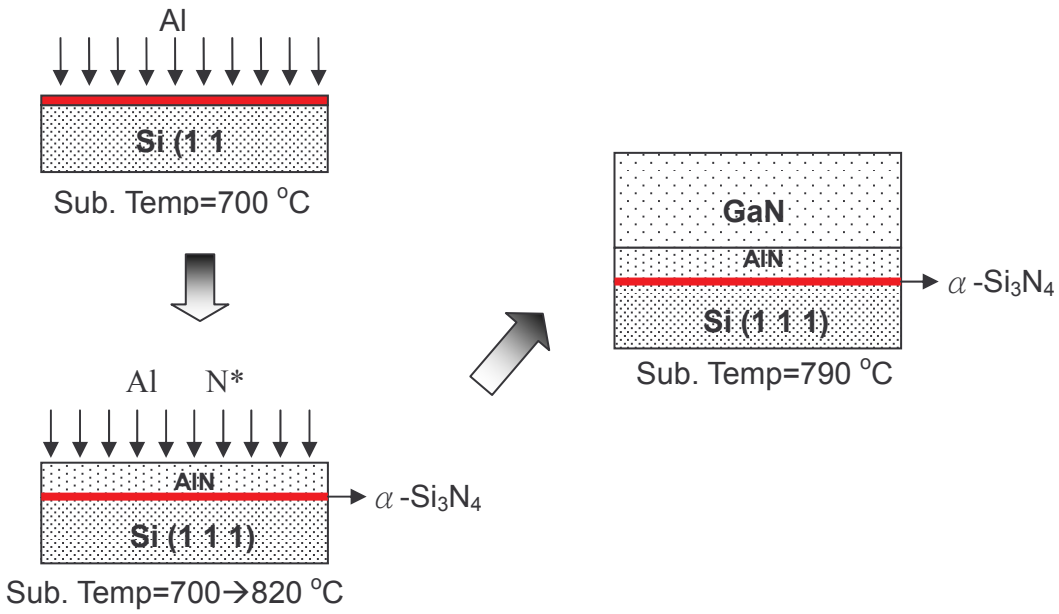

Fig. 4-1 Schematically depicts the growth procedure of GaN epilayer on Si (1 1 1) by using simultaneous AlN/α-Si_3N_4 buffer structure.

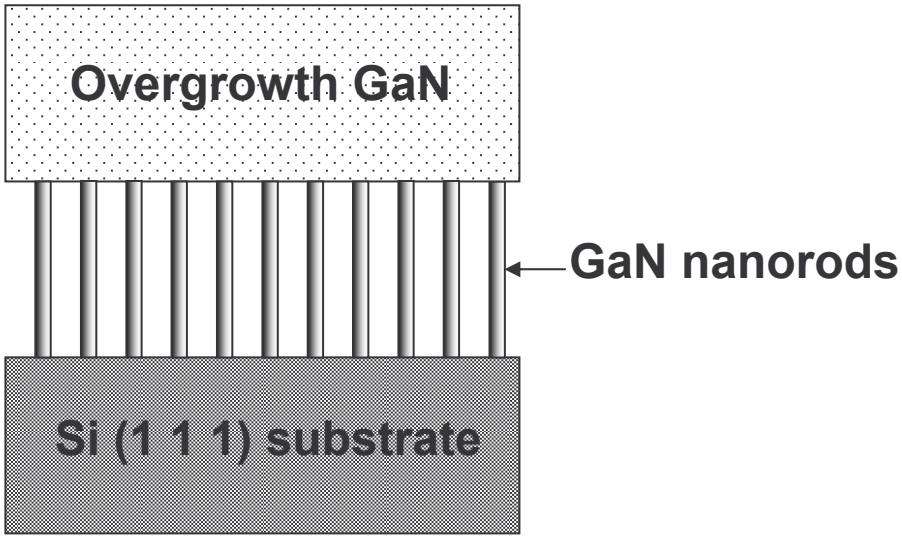

Fig. 4-2 Schematic diagrams of the overgrown GaN on self-assembled GaN nanorods

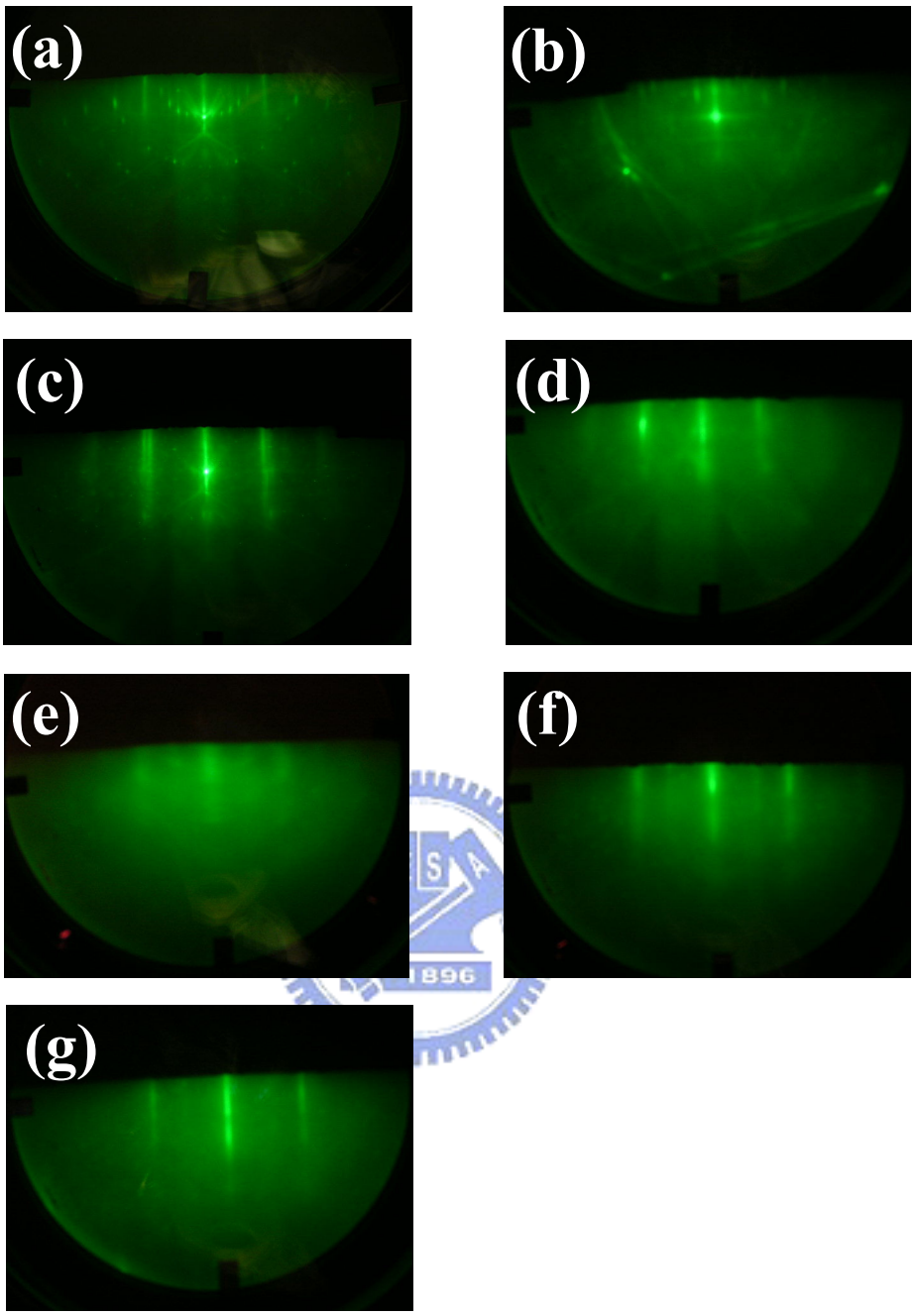

Fig. 4-3 The RHEED pattern of (a) the Si (1 1 1) 7×7 surface, (b) to (d) 15s, 30s, 45s Al pre-seeding layer deposition, (e) AlN without Al pre-seeding layer after 600s growth, (f) AlN with 45s Al pre-seeding layer after 600s growth and (g) the streaky (1×1) GaN RHEED pattern (45s Al pre-seeding layer).

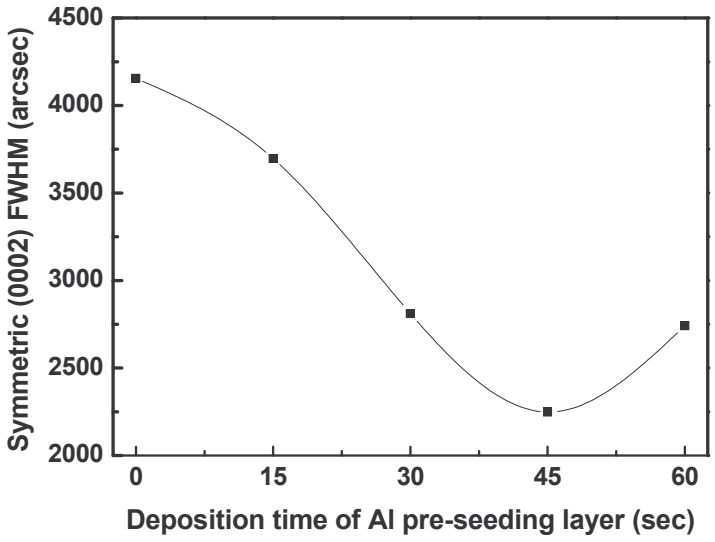

Fig. 4-4 FWHM of the x-ray rocking curve for the symmetric (0002) diffraction of GaN epilayer layer with various deposition time of Al pre-seeding layer.

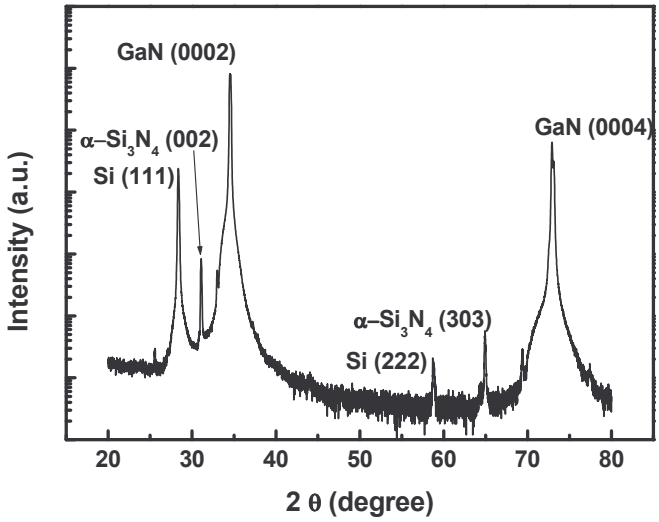

Fig. 4-5 XRD in the θ-2θ scan mode obtained from a GaN with α-Si_3N_4/AlN buffer structure on Si (1 1 1) substrate (45s Al pre-seeding layer).

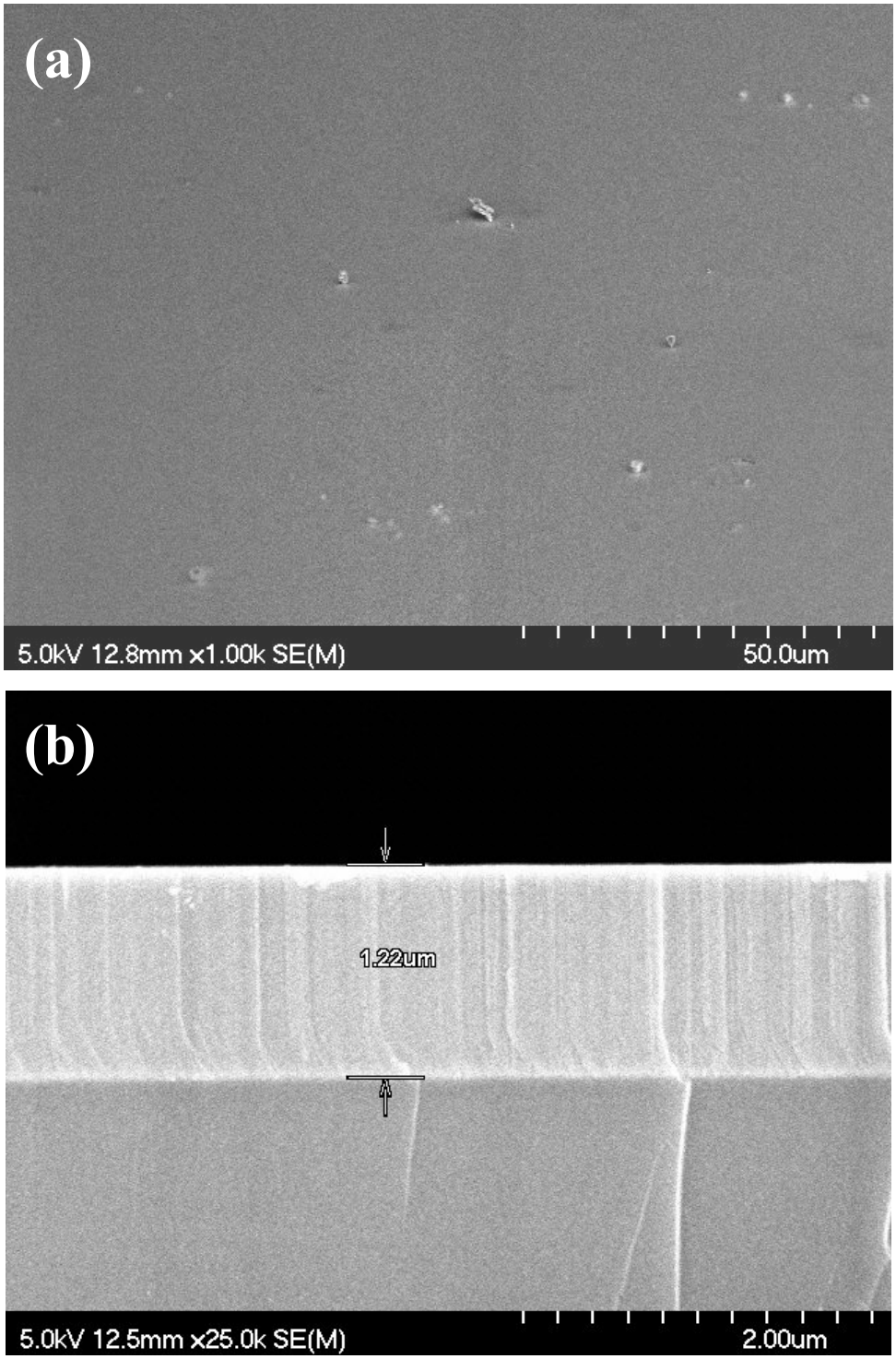

Fig. 4-6 SEM surface image of the GaN epitaxial layer on Si (1 1 1) with AlN/α-Si_3N_4 structure (45s Al pre-seeding layer), (a) plane view and (b) cross-section view.

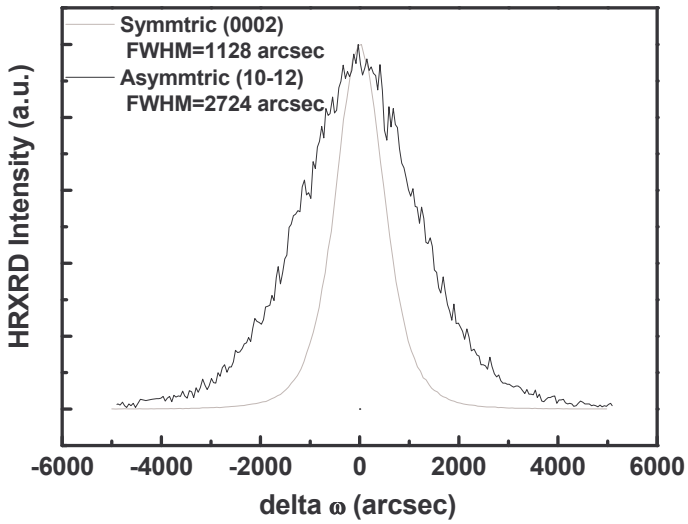

Fig. 4-7 Symmetric (0 0 0 2) and asymmetric (1 0 $\bar{1}$ 2) diffraction x-ray rocking curve of GaN epitaxial layer on Si (1 1 1) with AlN-IL (45s Al pre-seeding layer).

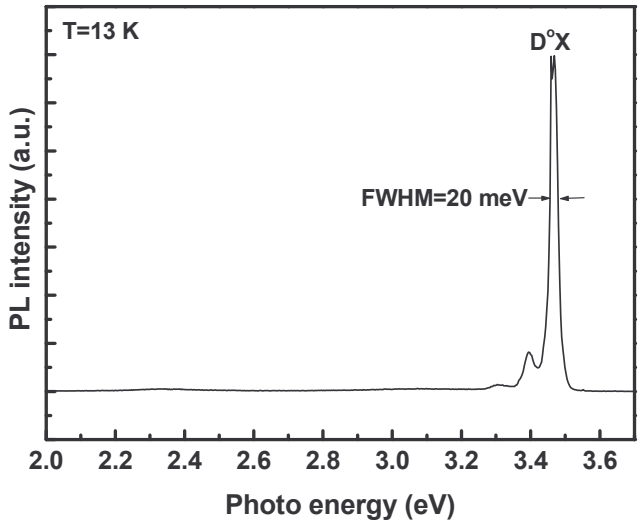

Fig. 4-8 PL of the GaN epitaxial layer on Si (1 1 1) with AlN-IL (45s Al pre-seeding layer) measured at 13K.

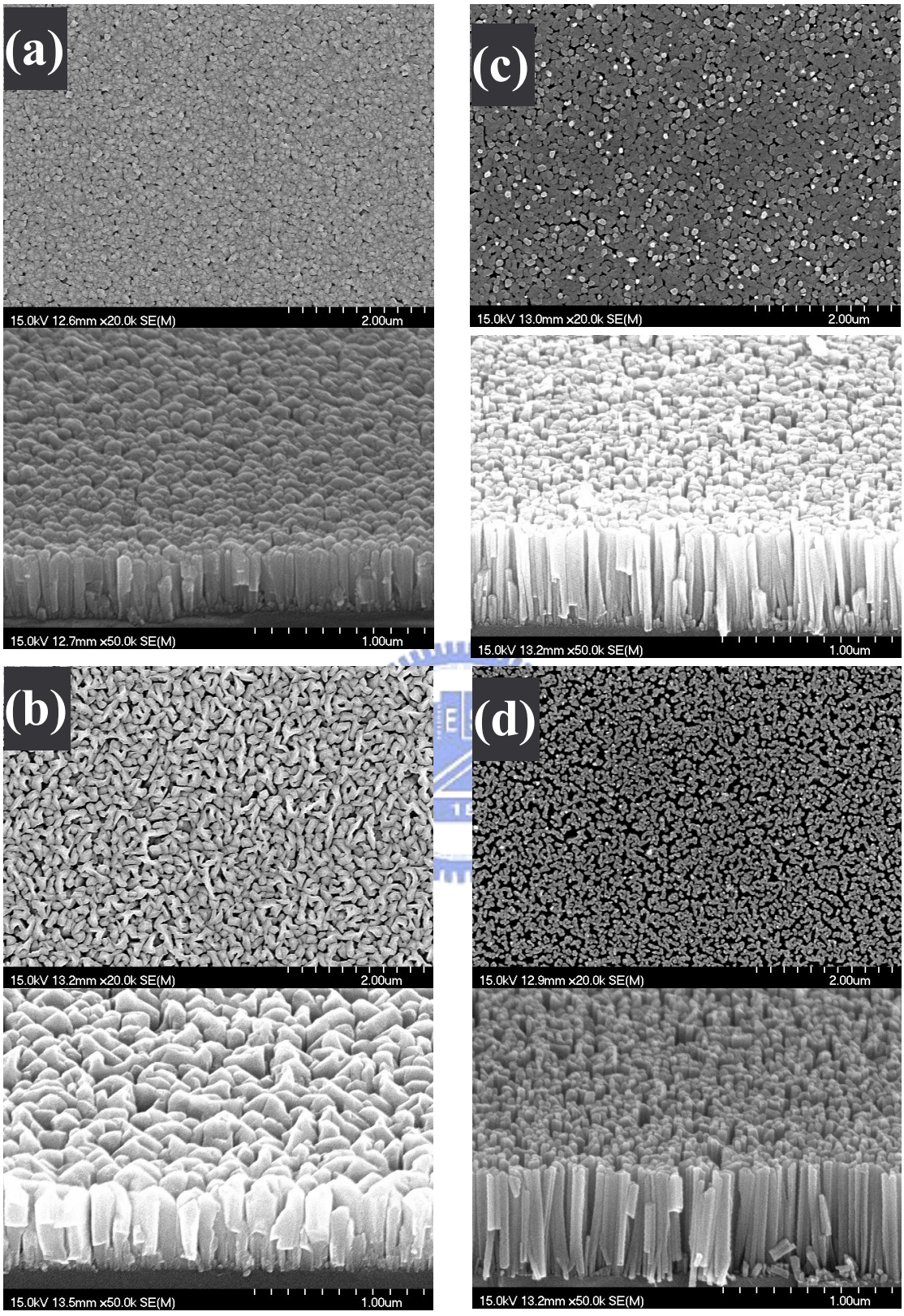

Fig. 4-9 SEM images of the self-assembled GaN nanorod grown on Si (1 1 1). Plan view and cross-section view of (a) Sub. Temp.=750 ℃ (b) Sub. Temp.=800 ℃ (c) Sub. Temp.=850 ℃ (d) Sub. Temp.=900 ℃.

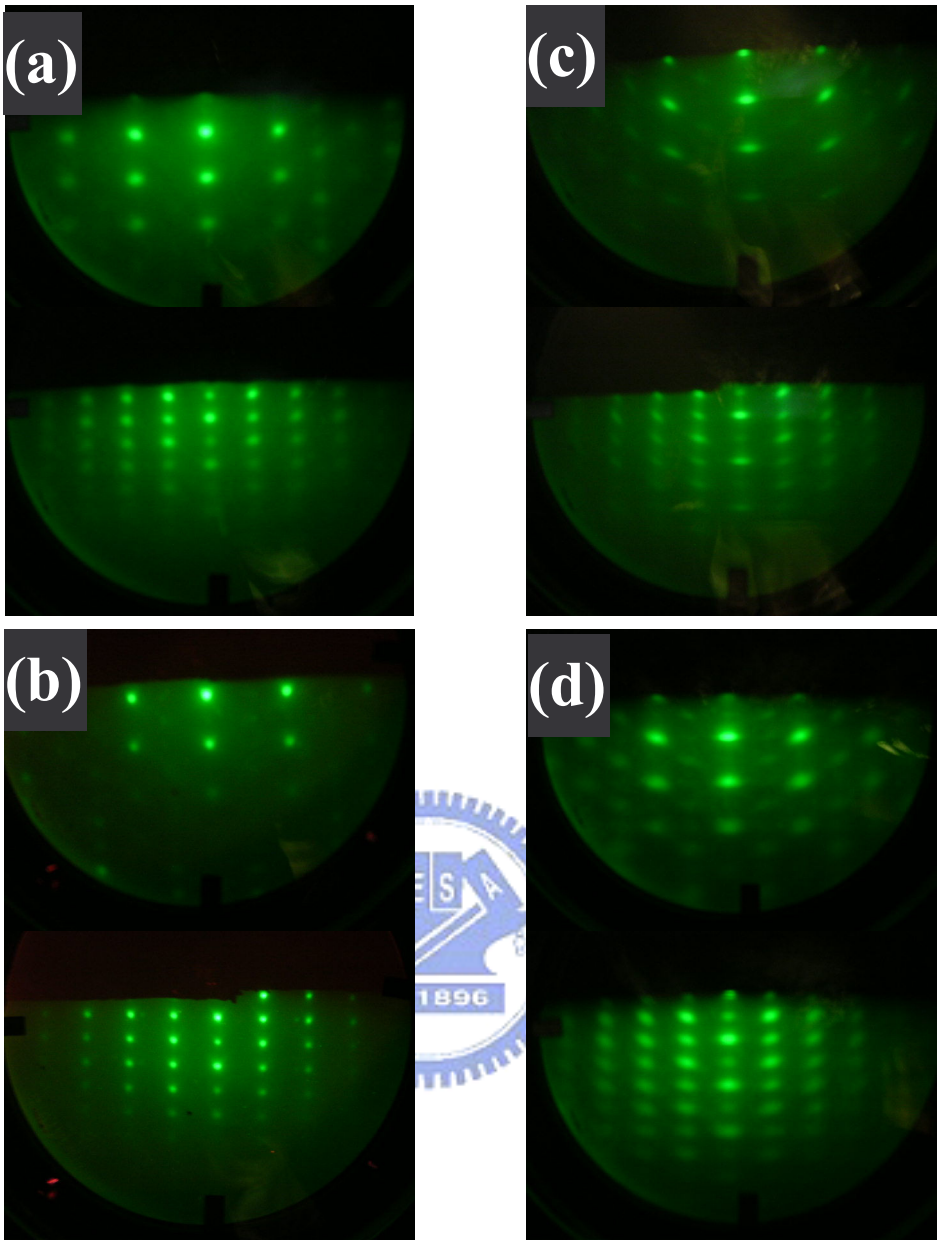

Fig. 4-10 The RHEED pattern along the <1-100> azimuth (Top pattern) and <2-1-10> azimuth (Bottom pattern) during the GaN nanorod growth of (a) Sub. Temp.=750 ℃ (b) Sub. Temp.=800 ℃ (c) Sub. Temp.=850 ℃ (d) Sub. Temp.=900 ℃

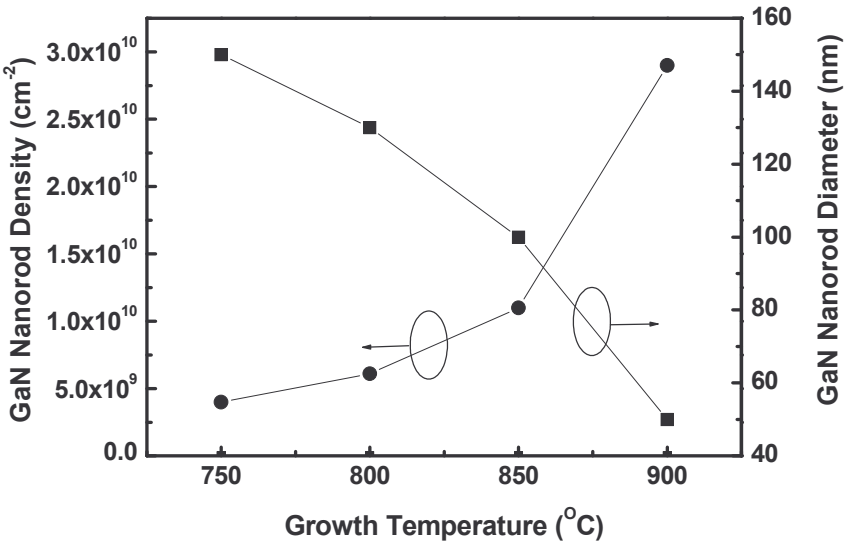

Fig. 4-11 Dependence of the GaN nanorod density and diameter on the growth temperature.

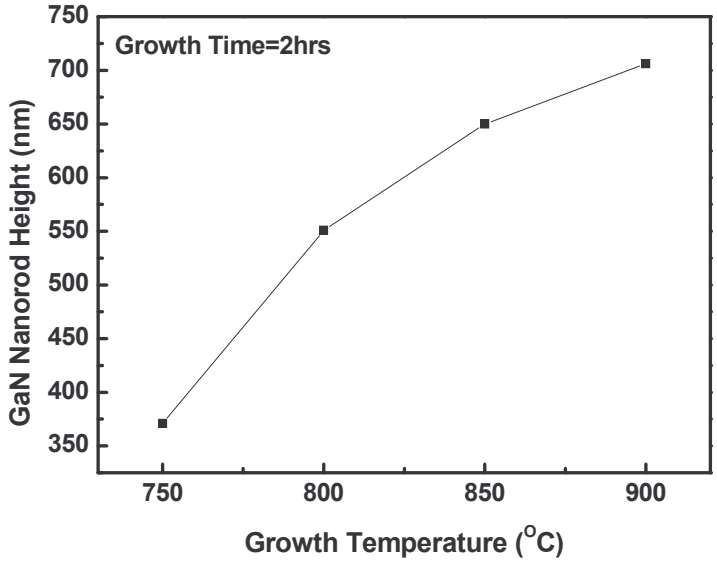

Fig. 4-12 The height of GaN nanorods as function of the growth temperature.

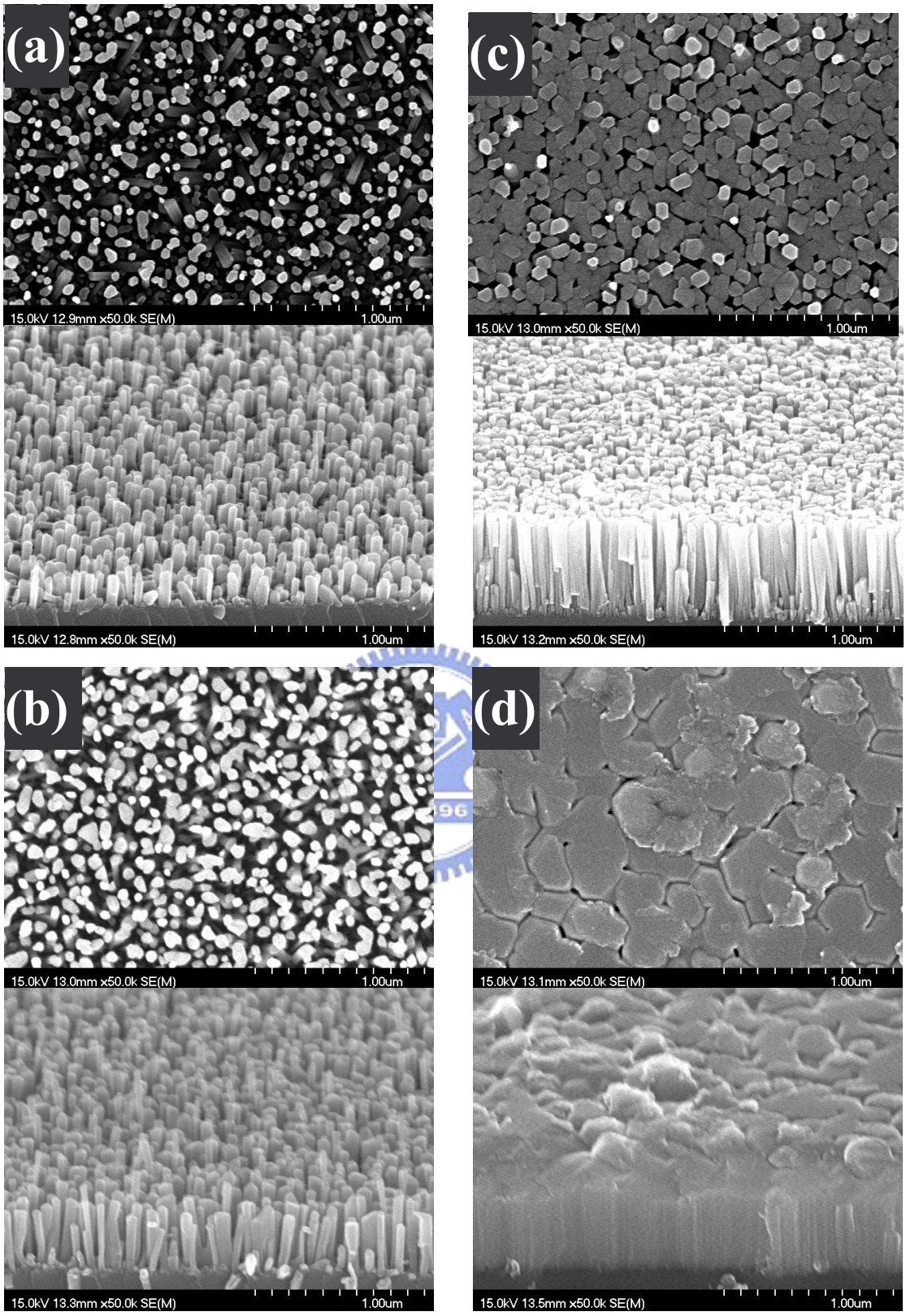

Fig. 4-13 SEM images of the self-assembled GaN nanorod grown on Si (1 1 1). Plan view and cross-section view of the BEP of (a) Ga=2.8×10^{-8}torr (b) Ga=7.1×10^{-8}torr (c) Ga=2.0×10^{-7}torr (d) Ga=3.6×10^{-7}torr.

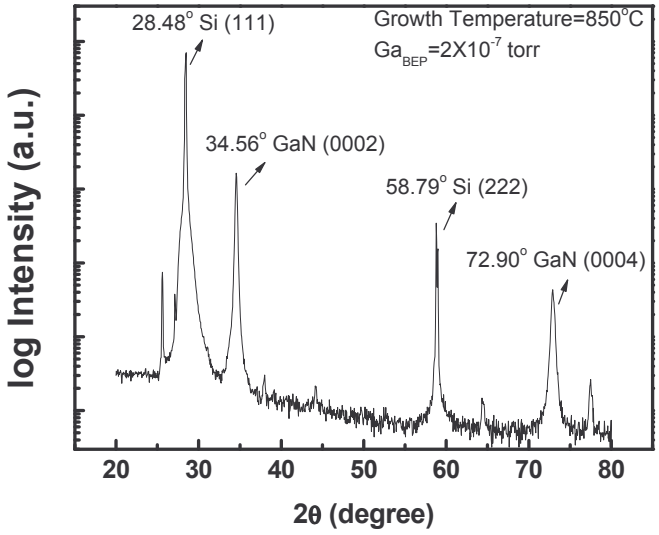

Fig. 4-14 XRD in the θ -2 θ scan mode of self-assembled nanorods in growth temperature=850℃.

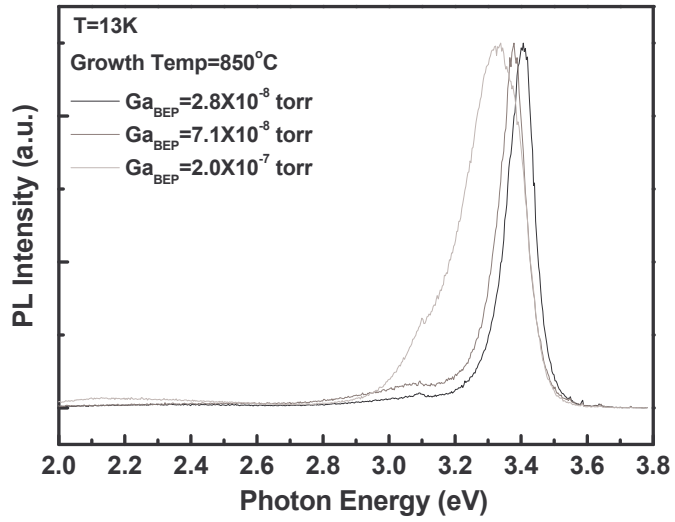

(a)

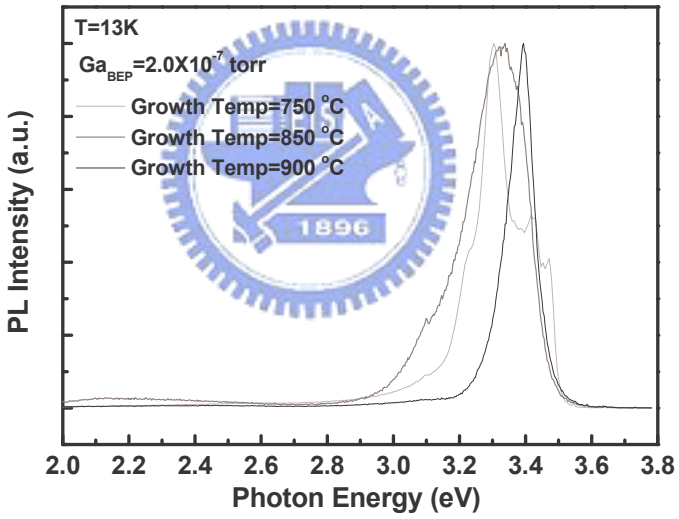

(b)

Fig. 4-15 PL spectra of the GaN nanorods with different (a) Ⅴ/Ⅲ ratio and (b) growth temperature.

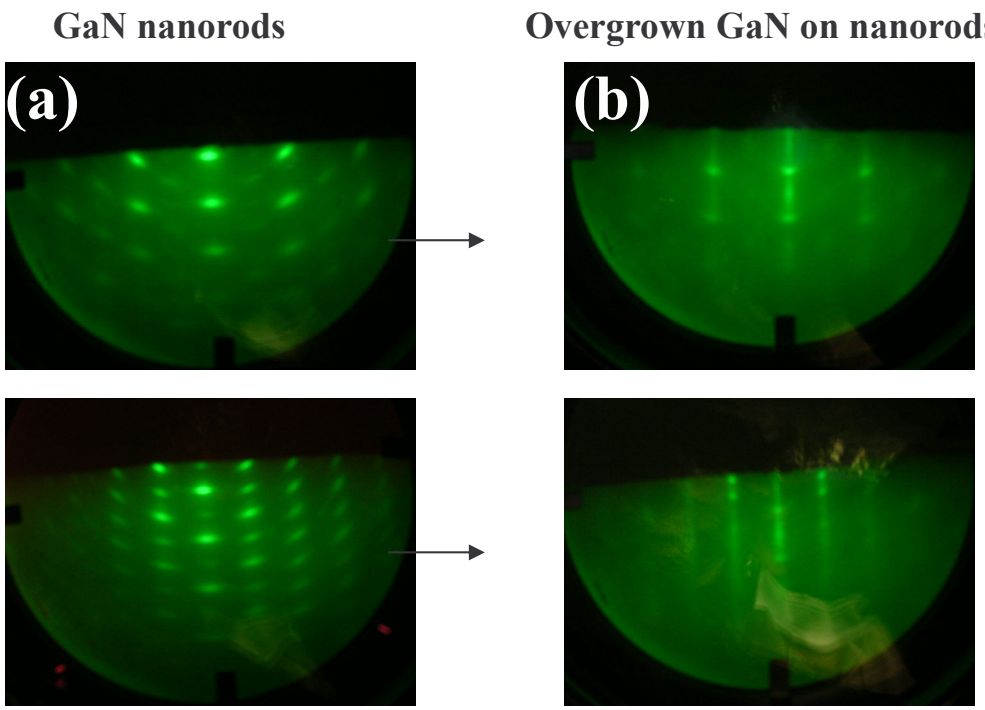

Fig. 4-16 The RHEED pattern along the <1-100> azimuth (Top pattern) and <2-1-10> azimuth (Bottom pattern) of (a) GaN nanorods, and (b) overgrown GaN.

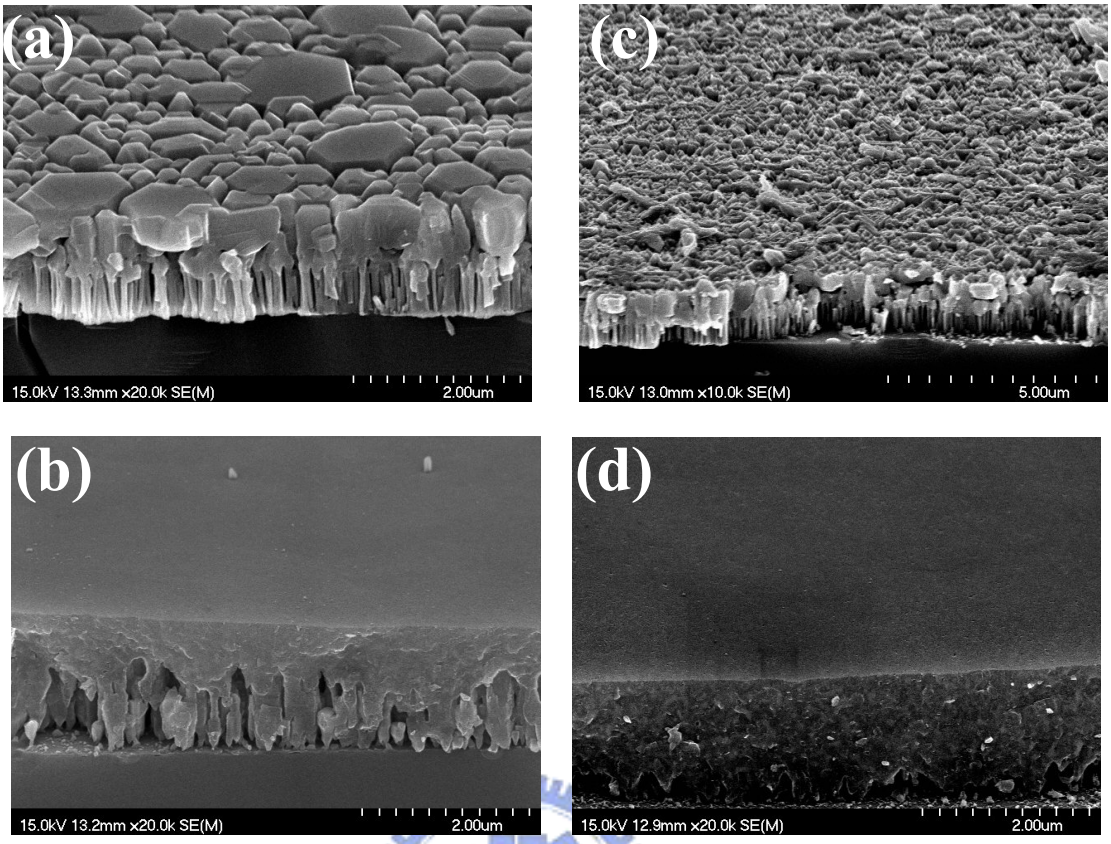

Fig. 4-17 SEM images of (a) MBE-overgrown and (b) MOCVD-overgrown GaN on self-assembled nanorods. After 2M KOH etch of (c) MBE-overgrown and (d) MOCVD-overgrown GaN.

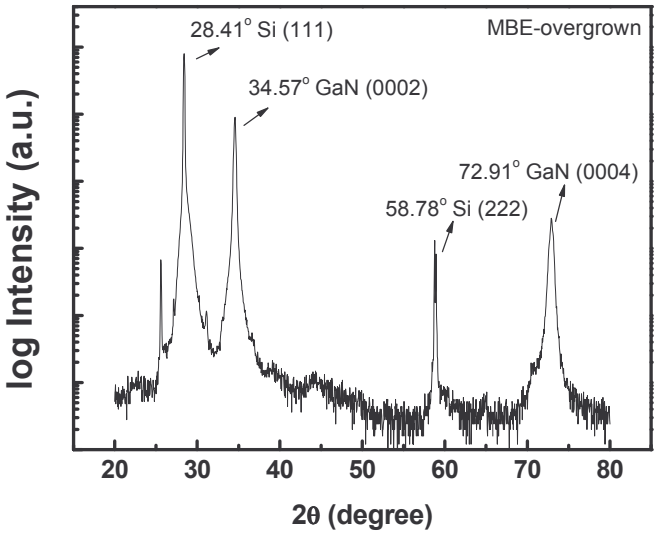

(a)

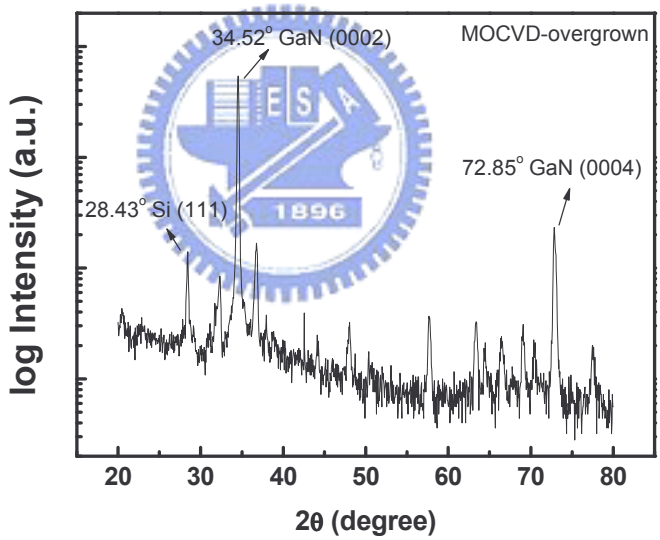

(b)

Fig. 4-18 XRD in the θ -2 θ scan mode of (a) MBE-overgrown and (b) MOCVD-overgrown GaN on the nanorods.

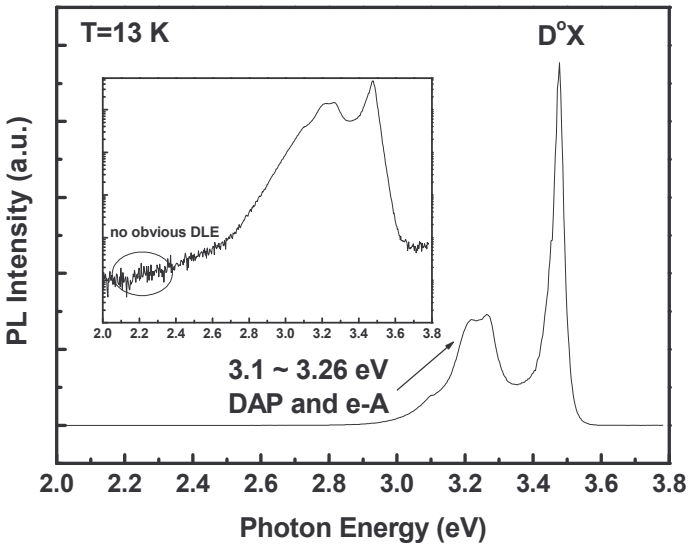

(a)

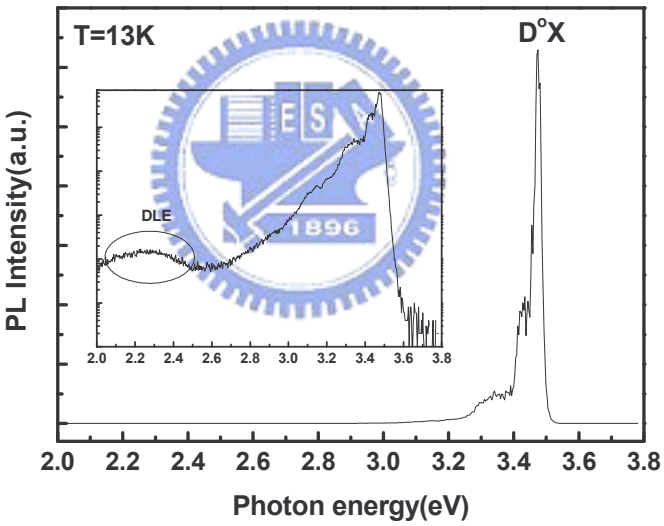

(b)

Fig. 4-19 PL spectra (linear scale) of the (a) MBE-overgrown and (b) MOCVD-overgrown GaN on self-assembled GaN nanorods. The insets are the PL spectra (log scale) of the overgrown GaN.